View metadata, citation and similar papers at core.ac.uk

brought to you by CORE

provided by Kyoto University Research Information Repository

Kyoto University Research Information Repository

KYOTO UNIVERSITY

Title	Selective etching of high-kk HfO[2] films over Si in hydrogen-added fluorocarbon (CF[4]／Ar／H[2] and C[4]F[8]／Ar／H[2]) plasmas
Author(s)	Takahashi, Kazuo; Ono, Kouichi
Citation	Journal of Vacuum Science & Technology A (2006), 24(3): 437-443
Issue Date	2006-04-20
URL	http://hdl.handle.net/2433/203170
Right	© 2006 American Vacuum Society. This article may be downloaded for personal use only. Any other use requires prior permission of the author and AIP Publishing. The following article may be found at http://scitation.aip.org/content/avs/journal/jvsta/24/3/10.1116/1.2187997
Type	Journal Article
Textversion	publisher

Kyoto University

Selective etching of high- k Hf O 2 films over Si in hydrogen-added fluorocarbon (C F 4 ∕Ar∕H 2 and C 4 F 8∕Ar∕H 2) plasmas

Kazuo Takahashi and Kouichi Ono

Citation: Journal of Vacuum Science & Technology A **24**, 437 (2006); doi: 10.1116/1.2187997
View online: http://dx.doi.org/10.1116/1.2187997
View Table of Contents: http://scitation.aip.org/content/avs/journal/jvsta/24/3?ver=pdfcov
Published by the AVS: Science & Technology of Materials, Interfaces, and Processing

Articles you may be interested in
SiCl4/Cl2 plasmas: A new chemistry to etch high-k materials selectively to Si-based materials
J. Vac. Sci. Technol. A **30**, 020602 (2012); 10.1116/1.3679551

Effects of in situ N 2 plasma treatment on etch of Hf O 2 in inductively coupled Cl 2∕N 2 plasmas
J. Vac. Sci. Technol. A **25**, 592 (2007); 10.1116/1.2731361

Dry etching of Ta N∕Hf O 2 gate-stack structure in B Cl 3∕Ar∕O 2 inductively coupled plasmas
J. Vac. Sci. Technol. A **24**, 1373 (2006); 10.1116/1.2210944

Etching characteristics of high- k dielectric Hf O 2 thin films in inductively coupled fluorocarbon plasmas
J. Vac. Sci. Technol. A **23**, 1691 (2005); 10.1116/1.2073468

Surface reaction of CF 2 radicals for fluorocarbon film formation in SiO 2 /Si selective etching process
J. Vac. Sci. Technol. A **16**, 233 (1998); 10.1116/1.580977

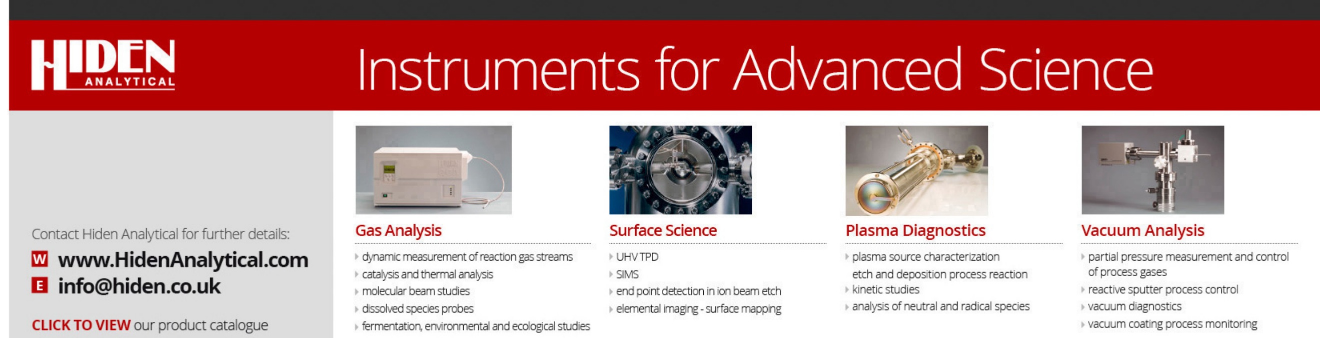

Redistribution subject to AVS license or copyright; see http://scitation.aip.org/termsconditions. Download to IP: 130.54.110.32 On: Mon, 25 Jan 2016 04:23:40

Selective etching of high-*k* HfO_2 films over Si in hydrogen-added fluorocarbon ($CF_4/Ar/H_2$ and $C_4F_8/Ar/H_2$) plasmas

Kazuo Takahashi[a] and Kouichi Ono
Department of Aeronautics and Astronautics, Kyoto University, Yoshida-Honmachi, Sakyo-ku, Kyoto 606-8501, Japan

(Received 3 June 2005; accepted 23 February 2006; published 20 April 2006)

Inductively coupled hydrogen-added fluorocarbon ($CF_4/Ar/H_2$ and $C_4F_8/Ar/H_2$) plasmas were used to etch HfO_2, which is a promising high-dielectric-constant material for the gate of complementary metal-oxide-semiconductor devices. The etch rates of HfO_2 and Si were drastically changed depending on the additive-H_2 flow rate in $C_4F_8/Ar/H_2$ plasmas. The highly selective etching of HfO_2 over Si was done in the condition with an additive-H_2 flow rate, where the Si surface was covered with the fluorocarbon polymer. The results of x-ray photoelectron spectroscopy indicated that the carbon content of the selectively etched HfO_2 surface was extremely low compared with the preetched surface contaminated by adventitious hydrocarbon in atmosphere. In the gas phase of the $C_4F_8/Ar/H_2$ plasmas, Hf hydrocarbide molecules such as metal-organic compounds and Hf hydrofluoride were detected by a quadrupole mass analyzer. These findings indicate that the fluorine species, carbon, and hydrogen can work to etch HfO_2 and that the carbon species also plays an important role in selective etching of HfO_2 over Si. *© 2006 American Vacuum Society.* [DOI: 10.1116/1.2187997]

I. INTRODUCTION

As dimensions of metal-oxide-semiconductor field-effect transistor (MOSFET) devices are scaled down in integrated circuits, the gate width will shrink to much less than 100 nm. The thickness of gate dielectrics should be reduced down to 2 nm or less for the present material, SiO_2.[1] Then, the thickness reduction of SiO_2 brings a number of serious problems such as increased gate-leakage current and reduced oxide reliability. Therefore, it will be necessary to integrate the high-dielectric-constant (k) materials, which can give higher specific capacitance at a larger thickness than SiO_2 and which enable the reduction of gate-leakage current. Integration of high-*k* materials will be one of the important issues in scaling MOSFET devices at critical dimensions below 65 nm.

Recently, replacing SiO_2 with silicon oxynitrides of slightly higher dielectric constant has been tried. In the future, high-*k* (>20) dielectrics or metal oxides such as HfO_2,[2] ZrO_2,[3,4] $HfSi_xO_y$,[5,6] and $ZrSi_xO_y$ (Refs. 6 and 7) will be developed to replace SiO_2. When integrating these materials into devices, these materials must be removed completely from the source and drain regions. Therefore, an understanding of the etch characteristics of high-*k* materials is required for the removal process.

Plasma etching of high-*k* materials has been studied recently for gate dielectric applications. Pelhos *et al.* reported on the etching of high-*k* gate dielectric $Zr_{1-x}Al_xO_y$ thin films with helical-resonator plasmas in Cl_2/BCl_3.[8] Sha *et al.* reported on the etching of ZrO_2 with electron-cyclotron-resonance plasmas in Cl_2 and BCl_3/Cl_2.[9,10] Furthermore, Sha *et al.* also etched HfO_2 thin films in the chlorine chemistries.[11,12] In their studies of HfO_2 etching, chlorine-based chemistries (not fluorine) were chosen because the HfO_2 was prevented from etching in the CHF_3 plasmas where Hf fluoride compound can be formed as the sidewall mask.[13,14] Norasetthekul *et al.* reported on the etching of HfO_2 with inductively coupled plasmas in Cl_2/Ar, SF_6/Ar, and $CH_4/H_2/Ar$.[15] Maeda *et al.* tried to integrate a MOSFET with a HfO_2 dielectric by using etching in CF_4 and Cl_2/HBr-based chemistries.[16] Emphasis in these studies has been placed on etch chemistries giving the selectivity of more than 1 over the underlying Si substrate and on a better understanding of physics and chemistry for the etching.

The thickness of the gate dielectrics for next-generation MOSFET devices (in the 65-nm technology node and beyond) will be several nanometers. Therefore, selectivity to underlying layers or mask materials will be more important than etch rate in the gate process.[17] From the point of view of HfO_2/Si selectivity, highly selective etching can be achieved in fluorocarbon plasmas. We found that HfO_2 can be etched by fluorine and that the selectivity of HfO_2/Si can be more than 5 in C_4F_8/Ar plasmas.[18] In the plasmas, carbon species work as a surface inhibitor on Si not containing oxygen and contribute to obtaining the high selectivity.

To enhance selectivity of HfO_2/Si, HfO_2 etching should be enhanced and/or Si etching should be suppressed. In SiO_2/Si selective etching, fluorocarbon polymer deposited on the surface plays an important role in enhancing the selectivity. The H_2 addition has an effect on the polymer formation in fluorocarbon plasmas.[19–21] Such chemistries may also be applied to HfO_2/Si selective etching. This article presents results of the etching of HfO_2 thin films on Si substrates in inductively coupled hydrogen-added fluorocarbon ($CF_4/Ar/H_2$ and $C_4F_8/Ar/H_2$) plasmas. We discuss the etch

[a]Electronic mail: takahashi@kuaero.kyoto-u.ac.jp

Redistribution subject to AVS license or copyright; see http://scitation.aip.org/termsconditions. Download to IP: 130.54.110.32 On: Mon, 25 Jan 2016 04:23:40

mechanism of HfO_2 affected by H_2 addition in the plasmas compared with that of SiO_2, which is well known in previous works.[22]

II. EXPERIMENT

The samples for etching were 60-nm-thick HfO_2 films on Si substrates prepared by chemical vapor deposition, SiO_2 films formed by thermal oxidation, and bare Si. The samples were cleaved into 2-cm^2 pieces and attached to a 4-in.-diameter Si wafer, which was then clamped onto a wafer stage.

Etching experiments were performed in a low-pressure inductively coupled plasma (ICP) reactor supplied with 13.56-MHz rf power.[18] The reactor consisted of a grounded stainless-steel chamber 25 cm in diameter and 25 cm in height. The rf power was coupled to the plasma via a three-turn planar rf induction coil 15 cm in outer diameter that was positioned on a quartz window 20 cm in diameter and 1.2 cm in thickness located at the top side of the chamber. The wafer stage was 13 cm in diameter and located at the bottom side of the chamber, where a close-fitting ground shield surrounded the stage. The distance from the bottom edge of the rf coupling window to the wafer stage was 5 cm. Gas mixtures of $CF_4/Ar(/H_2)$, $C_4F_8/Ar(/H_2)$ and CH_4/Ar, and pure Ar were introduced into the reactor, which was evacuated to a base pressure $<1\times10^{-6}$ Torr. The gas pressure and flow rate were maintained at 20 mTorr and 5–300 SCCM (SCCM denotes cubic centimeter per minute at STP), respectively.

The discharge was established at a nominal rf power of 280 or 300 W, corresponding to net powers of the π-type matching circuit driving the induction coil. The wafer stage was capacitively coupled to a separate 13.56-MHz rf power supply for additional biasing; the rf bias power was varied between 10 and 150 W (net power), resulting in a dc self-bias voltage on the stage down to between −40 and −160 V.

Sample pieces covered with masks of Si wafer were etched for several minutes. Steps appearing on the sample pieces were measured by stylus profilometry. The chemical composition of the surface was analyzed by x-ray photoelectron spectroscopy (XPS) using Mg $K\alpha$ x-ray radiation and a pass energy of 50 eV at a takeoff angle of 90°. The plasma parameters (ion density, electron temperature, and plasma potential) were determined by using a cylindrical Langmuir probe located at 2 cm above the wafer stage. The optical emissions from the F atom ($3s^4P_{5/2}-3p^4D^0_{7/2}$, 685.6 nm), H atom ($2p^2P^0_{3/2}-3d^2D_{3/2}$, 656.3 nm), HF molecule (486 nm),[23–25] and Ar atom ($4s'[\frac{1}{2}]^0-4p'[\frac{1}{2}]$, 750.4 nm) were observed to understand the chemical reactions in the gas phase. The etch products were detected by quadrupole mass spectrometry. A commercial quadrupole mass analyzer (QMA) was mounted on the chamber. Gas-phase species were introduced to the differentially pumped analyzer through a 100 μm orifice. The orifice was placed 3 cm from the stage and 2 cm above the wafer surface.

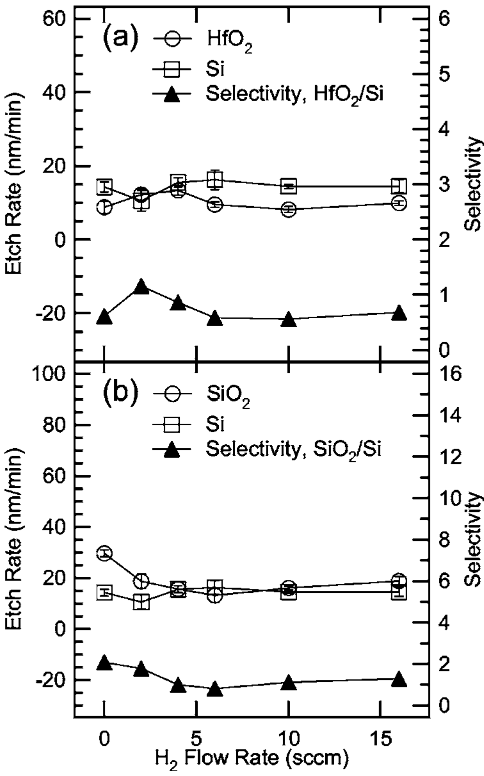

FIG. 1. Etch rates of (a) HfO_2 and (b) SiO_2 in $CF_4/Ar/H_2$ plasmas plotted with that of Si, and etch selectivities of (a) HfO_2/Si and (b) SiO_2/Si as a function of additive-H_2 flow rate. The rf bias power was constant at 50 W.

III. RESULTS AND DISCUSSION

A. Selective etching of HfO_2 over Si

Figure 1 shows the etch rates of (a) HfO_2 and (b) SiO_2 in $CF_4/Ar/H_2$ plasmas as a function of the additive-H_2 flow rate at constant rf powers of 280 W (to the coil) and 50 W (for bias), together with that of Si, and the etch selectivities of (a) HfO_2/Si and (b) SiO_2/Si. In generating the plasmas, the gas flow rates of CF_4 and Ar were 2.5 and 247.5 SCCM, respectively. The pressure was maintained at 20 mTorr. Figure 2 shows the etch rates of (a) HfO_2 and (b) SiO_2 in $C_4F_8/Ar/H_2$ plasmas. The gas flow rate of C_4F_8 was 2.5 SCCM. The other parameters were the same as in the $CF_4/Ar/H_2$ plasmas. The etch depth was measured as a function of etch time up to several minutes and exhibited an approximately linear increase with time. Thus, the etch rate was calculated as the ratio of the depth to time. In the figure, error bars correspond to variance in the measurements, which are not extended to calculating selectivities.

In the $CF_4/Ar/H_2$ plasmas, the etch rates of HfO_2, Si, and SiO_2 were maintained to be almost constant in all the tested H_2 flow rates. On the other hand, the etch rates of HfO_2 and Si in the $C_4F_8/Ar/H_2$ plasmas were drastically changed depending on H_2 flow rate. The fluorocarbon polymer was deposited on the Si surface between 4 and 8 SCCM in the H_2 flow rate. When H_2 is added to fluorocarbon plasmas, fluorine is scavenged by hydrogen with the production of the HF molecule in the gas phase,[26,27]

Redistribution subject to AVS license or copyright; see http://scitation.aip.org/termsconditions. Download to IP: 130.54.110.32 On: Mon, 25 Jan 2016 04:23:40

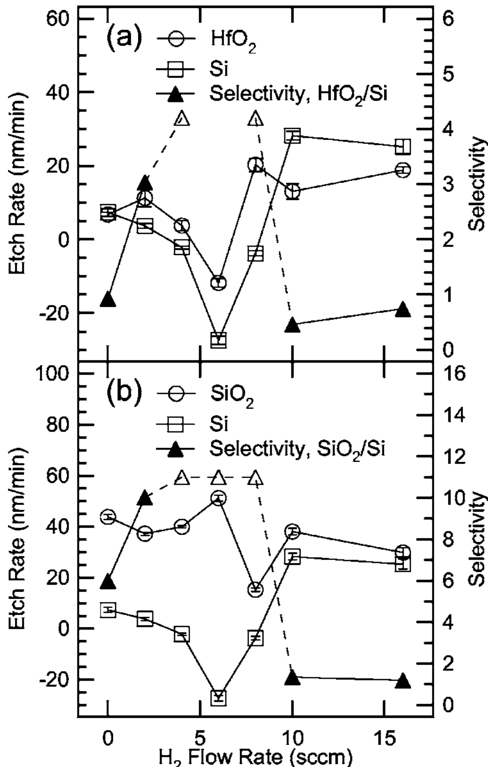

FIG. 2. Etch rates of (a) HfO_2 and (b) SiO_2 in $C_4F_8/Ar/H_2$ plasmas plotted with that of Si, and etch selectivities of (a) HfO_2/Si and (b) SiO_2/Si as a function of additive-H_2 flow rate. The rf bias power was constant at 50 W. At the conditions shown by the open triangle, complete selective etching of HfO_2 or SiO_2 was done.

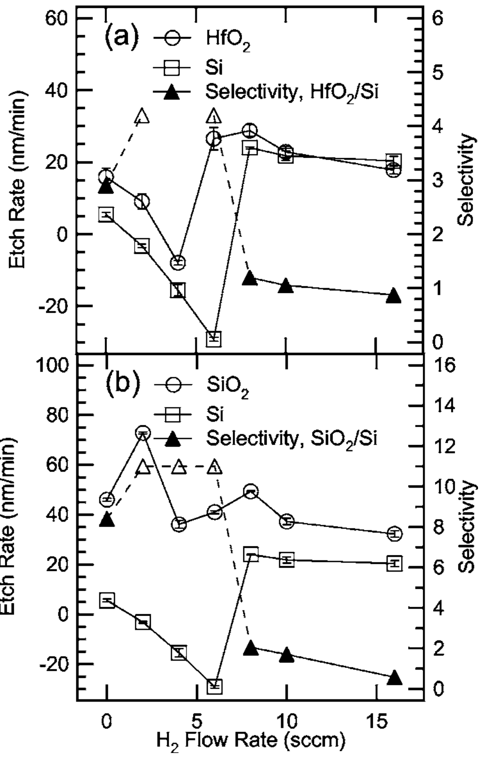

FIG. 3. Etch rates of (a) HfO_2 and (b) SiO_2 in $C_4F_8/Ar/H_2$ plasmas plotted with that of Si, and etch selectivities of (a) HfO_2/Si and (b) SiO_2/Si as a function of additive-H_2 flow rate. The self-bias voltage was maintained at −90 V.

$$C_xF_y + H \rightarrow C_xF_{y-1} + HF, \tag{1}$$

$$F + H \rightarrow HF. \tag{2}$$

Involving these reactions, the C/F ratio in fluorocarbon species becomes higher. The carbon-rich species are likely to have high sticking probability and to deposit on the surface. If the flow rate of CF_4 is increased, much more carbon-rich species are produced. Even in $CF_4/Ar/H_2$ plasmas, the species abundant in the gas phase can form deposited films.

At 6 SCCM in H_2 flow rate, the polymer also appeared on the HfO_2 surface in the $C_4F_8/Ar/H_2$ plasmas. At 4 and 8 SCCM, however, HfO_2 was etched selectively. In the case of a constant rf bias power, the self-bias voltage on the wafer stage was varied from −40 to −70 V with increasing additive-H_2 flow rate. The polymer formation on the surface can be affected by ion-bombarding energy changed with the self-bias voltage. Therefore, the etch characteristics were examined in the $C_4F_8/Ar/H_2$ plasmas at a constant self-bias voltage.

Figure 3 shows the etch rates in the plasmas where the self-bias voltage was maintained at a constant value of −90 V. The etch rates of HfO_2, Si, and SiO_2 were drastically changed between 0 and 6 SCCM in the H_2 flow rate and remained almost unchanged at flow rates more than 6 SCCM. The HfO_2 was etched selectively at 2 and 6 SCCM in the H_2 flow rate. Since the ion density was decreased with increasing H_2 flow rate from 0 to 6 SCCM (Fig. 4), the ion flux to the surface also decreased. The etching reactions of Si and fluorocarbon polymer on the surfaces seemed to be suppressed with decrease of the ion flux.

Optical-emission intensities of F, H, and Ar atoms and HF molecules were measured. It may be crucial to estimate the density of emitting species from the emission intensities. The intensity depends on many factors, such as electron density, electron energy-distribution function, density of the emitting species, excitation cross section of the excited state, and so on. Usually, actinometry is employed to quantify the density

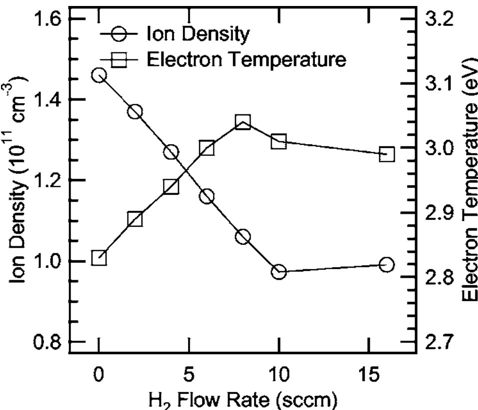

FIG. 4. Ion density and electron temperature determined in the Langmuir probe measurement as a function of additive-H_2 flow rate.

Redistribution subject to AVS license or copyright; see http://scitation.aip.org/termsconditions. Download to IP: 130.54.110.32 On: Mon, 25 Jan 2016 04:23:40

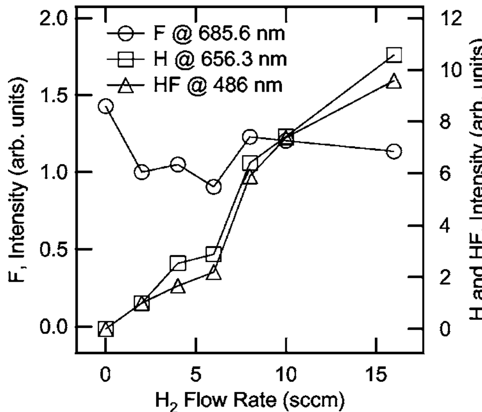

FIG. 5. Optical-emission intensities of F and H atoms and HF molecules as a function of additive-H_2 flow rate. These intensities were normalized by optical-emission intensity of Ar atoms.

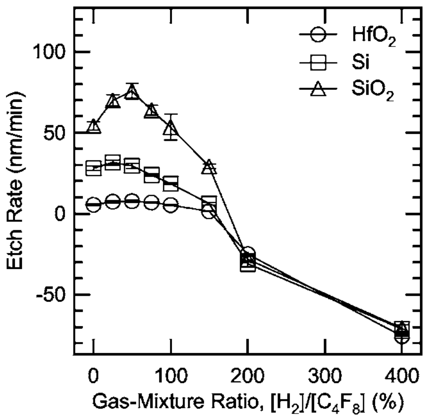

FIG. 6. Etch rates of HfO_2 and SiO_2 in C_4F_8/H_2 plasmas plotted with that of Si as a function of gas-mixture ratio of $[H_2]/[C_4F_8]$. The fluorocarbon gas flow rate, pressure, power to the coil, and self-bias voltage were maintained at 5 SCCM, 20 mTorr, 280 W, and −90 V, respectively.

of species by using noble gases.[28] In this work, all the optical-emission intensities were normalized by the emission intensity of Ar atoms at 750.4 nm. Figure 5 shows the normalized intensities of F and H atoms and HF molecules. Strictly speaking, since there is a difference in the electron excitation cross sections between the target species (F, H, and Ar atoms and HF molecules), the normalized intensities cannot represent quantitatively the density of the species. However, since the electron temperature (ranging between 2.8 and 3.0 eV in Fig. 4) was not changed significantly over the tested regime, the normalized intensities represent the qualitative trend in density for the species.

The density of H atoms increased with increasing H_2 flow rate. Especially, the density increased immediately between 6 and 8 SCCM in H_2 flow rate, where the reaction on the Si surface changed from deposition to etching. The F atoms were scavenged from fluorocarbon species and in the gas phase by H atoms from 2 to 6 SCCM in H_2 flow rate. The scavenging reaction reached saturation at 6 SCCM. The density of HF molecules increased with the increase of H atoms between 8 and 16 SCCM in the H_2 flow rate, where the H atom is abundant.

The density of F atoms between 2 and 6 SCCM in the H_2 flow rate became lower than that at 0 SCCM, since H atoms scavenged F atoms with the formation of HF molecules. Then, the density of F atoms was recovered between 8 and 16 SCCM, indicating that F atoms were produced by the electron-impact dissociation of HF molecules.[29,30] Thus, the etch rate of Si was decreased between 0 and 6 SCCM in the H_2 flow rate, with decreasing density of F atoms being an etchant for Si. In this regime, the deposition species, which were produced by the scavenging reaction of F, also reduced the etch rate of Si. The etch rate of SiO_2 was maintained, which can be etched by fluorocarbon species (including deposition species on Si surface) as well as by F atoms. Regarding the dissociation reaction of HF molecules, there are two possible paths:[29]

$$HF + e \rightarrow H + F + e, \quad (3)$$

$$H + HF^* \rightarrow H_2 + F, \quad (4)$$

where HF^* means vibrationally excited HF molecules, which can be present in hydrogen-added fluorine-containing discharges.[31–33]

Here we consider the role of H atoms in fluorocarbon plasmas. To elucidate the reaction of H atoms, the etch rates of HfO_2, Si, and SiO_2 were measured in C_4F_8/H_2 and CF_4/H_2 plasmas (shown in Figs. 6 and 7, respectively). The flow rates of C_4F_8 and CF_4 were 5 SCCM and that of H_2 was varied from 0 to 20 SCCM. The power to the coil and self-bias voltage were maintained at 280 W and −90 V, respectively. The pressure was set at 20 mTorr. In the C_4F_8/H_2 plasmas, the etching reaction occurred between 0% and 150% in the gas-mixture ratio of $[H_2]/[C_4F_8]$. The deposition film appeared at more than 150%. However, in CF_4/H_2 plasmas, the surface reactions on HfO_2 and Si were changed from etching to deposition with increasing gas-mixture ratio. Then the reactions were turned into etching again, since the

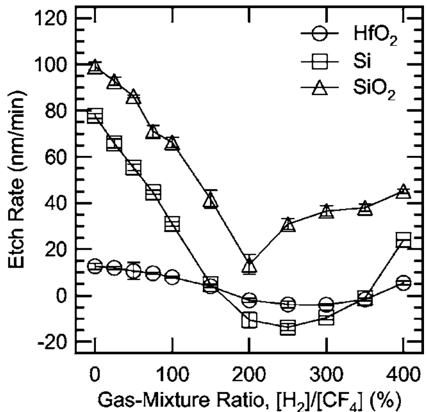

FIG. 7. Etch rates of HfO_2 and SiO_2 in CF_4/H_2 plasmas plotted with that of Si as a function of gas-mixture ratio of $[H_2]/[CF_4]$. The experimental parameters were the same as in Fig. 6.

Redistribution subject to AVS license or copyright; see http://scitation.aip.org/termsconditions. Download to IP: 130.54.110.32 On: Mon, 25 Jan 2016 04:23:40

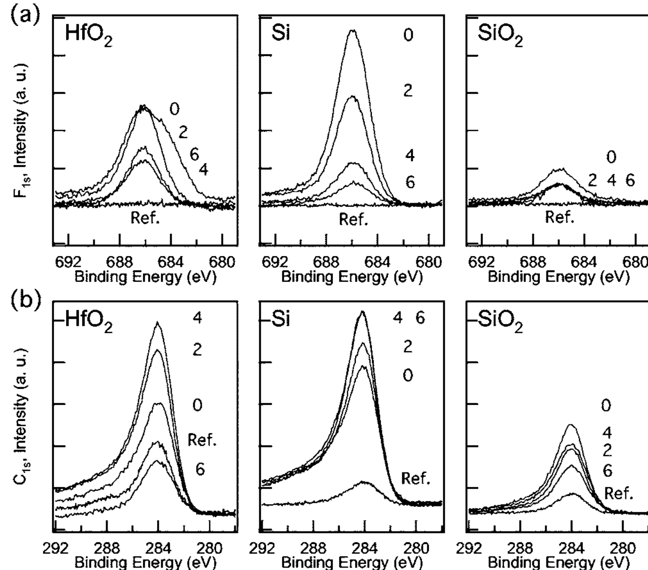

FIG. 8. XPS spectra of F_{1s} and C_{1s} on HfO_2, Si, and SiO_2 surfaces etched in the $C_4F_8/Ar/H_2$ plasmas and on preetched surfaces (indicated by notation of "Ref."). The experimental conditions were the same as in Fig. 3. The values of additive-H_2 flow rate from 0 to 6 SCCM are shown in the graphs.

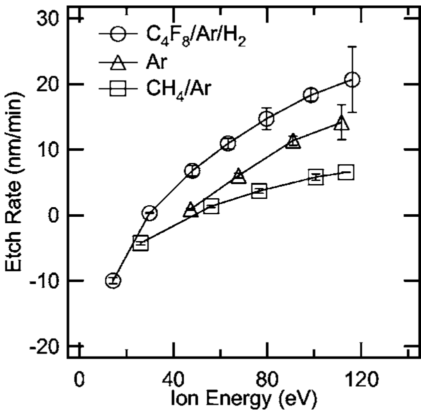

FIG. 9. Etch rates of HfO_2 in $C_4F_8/Ar/H_2$ (2.5/247.5/16 SCCM), pure Ar (250 SCCM), and CH_4/Ar (12.5/237.5 SCCM) plasmas as a function of ion energy. The pressure and power to the coil were maintained at 20 mTorr and 300 W, respectively.

deposition film was made thinner with H_2 addition. Furthermore, when the C_4F_8 flow rate is less than 5 SCCM, the thickness of the deposition film is thinner and the etching reaction can occur at more than 400% of the gas-mixture ratio. Therefore, it is essential that the reaction on the Si surface changes from etching to deposition and from deposition to etching with the addition of H_2 atoms. These facts show that the excess H atoms, which do not contribute to the production of HF molecules or are produced by the dissociation of HF molecules, can etch the deposition film of the fluorocarbon polymer. One can understand the etching of fluorocarbon polymer by H atoms by the analogy of the etching of graphite by H atoms in the process of diamond synthesis.[34] In Fig. 3, the etching of HfO_2 and Si can proceed from 8 to 16 SCCM in the H_2 flow rate, since etchants (including F atoms) can reach the HfO_2, Si, and SiO_2 surfaces, as a result of the etching of excess H atoms and removing of the deposition film of the fluorocarbon polymer.

Figure 8 shows the XPS spectra of F_{1s} and C_{1s} on HfO_2, Si, and SiO_2 etched in the $C_4F_8/Ar/H_2$ plasmas, and on preetched surfaces (indicated by notation of "Ref."). The experimental conditions were the same as in Fig. 3. In the figure, the numbers from 0 to 6 correspond to the additive-H_2 flow rate. The carbon content on preetched surfaces can be detected from the adventitious hydrocarbon of atmospheric contaminants. On SiO_2 surfaces, intensities of F_{1s} and C_{1s} signals were weak compared with other samples. This means that SiO_2 can be etched by various fluorocarbon species with the formation of volatile products containing F and C atoms. On Si surfaces, the spectra of 2, 4, and 6 SCCM in the additive-H_2 flow rate show the chemical composition of the deposition film of fluorocarbon polymer. The F content decreased and C content increased with the increased additive-H_2 flow rate, indicating that the deposition film became more carbon rich with the increasing additive-H_2 flow rate. On HfO_2 surfaces, especially, at 8 SCCM in the additive-H_2 flow rate, the intensity of the C_{1s} signal was extremely low, which was lower than that of the reference surface contaminated by adventitious hydrocarbon in atmosphere. Furthermore, the C/F ratio on the HfO_2 surface at 8 SCCM was lower than that of the fluorocarbon polymer film on Si surface. These facts imply that the etching of HfO_2 could proceed involving volatile etch products containing C atoms.

To understand species reactive with HfO_2, the etch characteristics of HfO_2 were examined in $C_4F_8/Ar/H_2$ (2.5/247.5/16 SCCM), pure Ar (250 SCCM), and CH_4/Ar (12.5/237.5 SCCM) plasmas. Figure 9 shows the etch rates in these plasmas. Here, the ion energy was defined by $|V_p - V_{dc}|$, where V_p and V_{dc} correspond to plasma potential measured by Langmuir probe and self-bias voltage, respectively. The power to the coil and pressure were maintained at 300 W and 20 mTorr, respectively. The ion densities in the $C_4F_8/Ar/H_2$, pure Ar, and CH_4/Ar plasmas were 1.5×10^{11}, 3.6×10^{11}, and 1.5×10^{11} cm^{-3}, respectively. The etch rates in the pure Ar plasmas did not exceed those in the $C_4F_8/Ar/H_2$ plasmas, although the ion density in the pure Ar plasmas was two times higher than that in the $C_4F_8/Ar/H_2$ plasmas. Therefore, the etching of HfO_2 can proceed with involving chemical reactions related to C, F, and H species in the $C_4F_8/Ar/H_2$ plasmas. In addition, the etch rates in the CH_4/Ar plasmas did not exceed those in the pure Ar plasmas and is not dependent on the CH_4 flow rate. The deposition of carbon species suppressed etching of HfO_2.

B. Volatile products in HfO_2 etching

As mentioned above, at least the F species is necessary to etch HfO_2. The carbon species may also play a role in the etching of HfO_2, as implied by the results of XPS measurements. Understanding the etch mechanism is one of the most important issues in knowing the etchants of HfO_2 in fluorocarbon plasmas. In this study, a QMA with a mass range from 0.4 to 500 amu was used to observe the ionic species

Redistribution subject to AVS license or copyright; see http://scitation.aip.org/termsconditions. Download to IP: 130.54.110.32 On: Mon, 25 Jan 2016 04:23:40

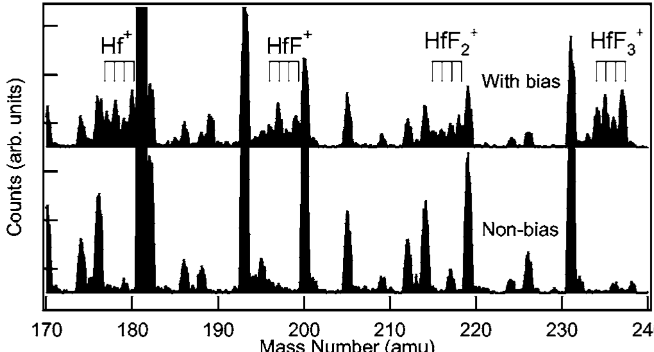

FIG. 10. Mass spectra of ionic species in C_4F_8/Ar plasmas. The species were observed in the cases without (upper graph indicated by "With bias") and with bias power (lower graph indicated by "Non-bias"). The HfO_2 was etched in the condition with bias power, resulting in self-bias voltage of −90 V.

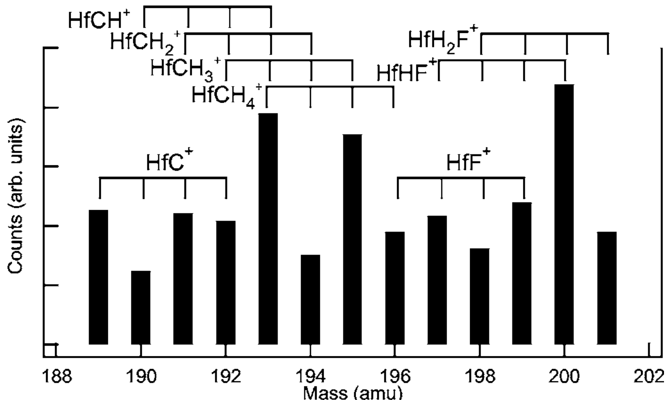

FIG. 11. Mass spectrum of ionic species as the etch products with mass range from 189 to 201 in $C_4F_8/Ar/H_2$ plasmas. The additive-H_2 flow rate, pressure, power to the coil, and self-bias voltage were set at 8 SCCM, 20 mTorr, 280 W, and −90 V (with biased condition). The spectrum was obtained by subtracting the spectrum in the nonbiased condition from that in the with biased condition where the HfO_2 could be selectively etched.

and the etch products in the gas phase. The ionic species were detected in the C_4F_8/Ar plasmas, where the C_4F_8 flow rate, pressure, and power to the coil were maintained at 2.5 SCCM (1% of the total), 20 mTorr, and 280 W, respectively (Fig. 10). The various ionic species of fluorocarbon were observed in the plasmas, including those with mass higher than the parent molecule (>200 amu). In the etching of HfO_2 with a self-bias voltage of −90 V, the ionic species as etch products were detected. The several peaks appearing in etching were assigned to Hf^+, HfF^+, HF_2^+, and HF_3^+ in the spectrum (Fig. 10), compared with the calculated mass patterns using the relative abundance of naturally occurring Hf isotopes,[35] i.e., ^{177}Hf (18.6%), ^{178}Hf (27.3%), ^{179}Hf (13.6%), and ^{180}Hf (35.1%). These Hf fluoride ions may be produced by the electron-impact dissociation of HfF_4. These cannot be identified to be the primary etch products, nor secondary or higher. It is certain that the Hf fluoride must be included in the etch products as volatile species.

In $C_4F_8/Ar/H_2$ plasmas, the etch products were also observed. The gas flow rates of C_4F_8, Ar, and H_2 were 2.5, 247.5, and 8 SCCM, respectively. The pressure, power to the coil, and self-bias voltage were set at 20 mTorr, 280 W, and −90 V, respectively. These experimental parameters correspond to the condition where HfO_2 can be selectively etched (Fig. 3) and where the etch products may contain C atoms, as implied by the XPS results (Fig. 8). Figure 11 shows the mass spectrum of ionic species with mass ranging from 189 to 201 amu. The spectrum was obtained by subtracting the spectrum in the nonbiased condition from that in the biased condition. Therefore, the spectrum indicates the contents of etch products only. The peaks of the contents can be assigned to $HfCH_x^+$ $(x=0-4)$ and HfH_xF^+ $(x=0-2)$. The peaks from 193 to 196 amu also correspond to HfO^+. Since these peaks were not observed in CF_4/Ar and C_4F_8/Ar plasmas, the peaks should be assigned to $HfCH_4^+$, whose molecular structure is unknown. Since the molecules of Hf carbide were detected as etch products, a carbon-poor surface prepared in $C_4F_8/Ar/H_2$ plasmas with an additive-H_2 flow rate of 8 SCCM was formed in etching reactions involving carbon species.

The $HfCH_x^+$ and HfH_xF^+ may be produced by the dissociation of molecules with the structure like metal-organic compounds. Although HfC^+ was detected, the molecule may be produced from $HfCH_x^+$, since the yield of C atoms is too low to etch HfO_2.[36] It may be natural that HfO_2 is etched with the production of metal-organic compounds as etch products, since such compounds are used for chemical vapor deposition of HfO_2.[37–39] In addition, it may be possible to etch HfO_2 by CH_4 chemistries with optimized experimental parameters, although the results in CH_4/Ar plasmas (Fig. 9) could not prove this possibility in the present work.

IV. CONCLUSION

In the present study, the etch characteristics of HfO_2 were examined in $CF_4/Ar/H_2$ and $C_4F_8/Ar/H_2$ plasmas. When H_2 was added to the C_4F_8/Ar plasmas, the highly selective etching of HfO_2 over Si could be done. The HfO_2 was etched even in the condition where fluorocarbon polymer film was deposited on a Si surface.

On the HfO_2 surface etched selectively in the $C_4F_8/Ar/H_2$ plasmas, the carbon content was lower than the adventitious hydrocarbon of the atmospheric contaminant on the preetched surface. This implied that the carbon and/or hydrocarbon species may be etchants of HfO_2 and the etch products may contain Hf and carbon atoms. The sputtering rates of HfO_2 in pure Ar plasmas did not exceed the etch rates in the $C_4F_8/Ar/H_2$ plasmas and were higher than the etch rates in CH_4/Ar plasmas. Therefore, fluorine species are necessary to etch HfO_2 in our examples. In the gas phase, $HfCH_x^+$ $(x=0-4)$ and HfH_xF^+ $(x=0-2)$ were detected by QMA. The Hf hydrocarbidelike metal-organic compound was determined to be one of the volatile etch products in the $C_4F_8/Ar/H_2$ plasmas. The formation of metal-organic compounds is an interesting topic for the etching and depositing of materials containing transition metals. Further analyses will be important for the materials introduced to next-generation devices.

Redistribution subject to AVS license or copyright; see http://scitation.aip.org/termsconditions. Download to IP: 130.54.110.32 On: Mon, 25 Jan 2016 04:23:40

In the actual gate processes, the highly selective etching of HfO_2 over Si can be performed with precise control of H_2 addition in $C_4F_8/Ar/H_2$ plasmas. The polymer deposition brought by H_2 addition is effective for reducing the etch rate of Si. Furthermore, the polymer may even prevent etching of HfO_2 in narrow trenches of musks. Therefore, for practical use, the experimental parameters such as additive-H_2 flow rate should be optimized while observing the etch profiles.

ACKNOWLEDGMENTS

This work was supported by the New Energy and Industrial Technology Development Organization (NEDO)/Millennium Research for Advanced Information Technology (MIRAI) project.

[1]*The International Technology Roadmap of Semiconductor*, 2001 ed. (International Sematech, Austin, TX, 2001).
[2]Y.-S. Lin, R. Puthenkovilakam, and J. P. Chang, Appl. Phys. Lett. **81**, 2041 (2002).
[3]J. P. Chang, Y.-S. Lin, S. Berger, A. Kepten, R. Bloom, and S. Levy, J. Vac. Sci. Technol. B **19**, 2137 (2001).
[4]M. Copel, M. Gribelyuk, and E. Gusev, Appl. Phys. Lett. **76**, 436 (2000).
[5]G. D. Wilk and R. M. Wallace, Appl. Phys. Lett. **74**, 2854 (1999).
[6]G. D. Wilk, R. M. Wallace, and J. M. Anthony, J. Appl. Phys. **87**, 484 (2000).
[7]W.-J. Qi, R. Nieh, E. Dharmarajan, B. H. Lee, Y. Jeon, L. Kang, K. Onishi, and J. C. Lee, Appl. Phys. Lett. **77**, 1704 (2000).
[8]K. Pelhos *et al.*, J. Vac. Sci. Technol. A **19**, 1361 (2001).
[9]L. Sha, B.-O. Cho, and J. P. Chang, J. Vac. Sci. Technol. A **20**, 1525 (2002).
[10]L. Sha and J. P. Chang, J. Vac. Sci. Technol. A **21**, 1915 (2003).
[11]L. Sha, R. Puthenkovilakam, Y.-S. Lin, and J. P. Chang, J. Vac. Sci. Technol. B **21**, 2420 (2003).
[12]L. Sha and J. P. Chang, J. Vac. Sci. Technol. A **22**, 88 (2004).
[13]K. K. Shih, T. C. Chieu, and D. B. Dove, J. Vac. Sci. Technol. B **11**, 2130 (1993).
[14]J. A. Britten, H. T. Nguyen, S. F. Falabella, B. W. Shore, and M. D. Perry, J. Vac. Sci. Technol. A **14**, 2973 (1996).
[15]S. Norasetthekul *et al.*, Appl. Surf. Sci. **187**, 75 (2002).
[16]T. Maeda *et al.*, Jpn. J. Appl. Phys., Part 1 **43**, 1864 (2004).
[17]K. Ono, 2004 Semiconductor Technology Outlook (unpublished), p. 331 (in Japanese).
[18]K. Takahashi, K. Ono, and Y. Setsuhara, J. Vac. Sci. Technol. A **23**, 1691 (2005).
[19]L. M. Ephrath, J. Electrochem. Soc. **126**, 1419 (1979).
[20]J. W. Coburn, J. Appl. Phys. **50**, 5210 (1979).
[21]G. S. Oehrlein and H. L. Williams, J. Appl. Phys. **62**, 662 (1987).
[22]M. Sekine, Appl. Surf. Sci. **192**, 270 (2002).
[23]R. G. Frieser and J. Nogay, Appl. Spectrosc. **34**, 31 (1980).
[24]M. M. Millard and E. Kay, J. Electrochem. Soc. **129**, 160 (1982).
[25]R. d'Agostino, F. Cramarossa, and S. De Benedictis, Plasma Chem. Plasma Process. **4**, 21 (1984).
[26]C.-P. Tsai and D. L. McFadden, J. Phys. Chem. **93**, 2471 (1989).
[27]M. A. Ioffe, Y. M. Gershenzon, V. B. Rozenshtein, and S. Y. Umanskii, Chem. Phys. Lett. **154**, 131 (1989).
[28]J. W. Coburn and M. Chen, J. Appl. Phys. **51**, 3134 (1980).
[29]R. d'Agostino, F. Cramarossa, V. Colaprico, and R. d'Ettole, J. Appl. Phys. **54**, 1284 (1983).
[30]Y. Hikosaka, M. Nakamura, and H. Sugai, Jpn. J. Appl. Phys., Part 1 **33**, 2157 (1994).
[31]O. D. Krogh and G. C. Pimentel, J. Chem. Phys. **67**, 2993 (1977).
[32]L. Bertrand, J. M. Gagne, B. Mongeau, B. Lapointe, Y. Conturie, and M. Moisan, J. Appl. Phys. **48**, 224 (1977).
[33]L. Bertrand, J. M. Gagne, R. G. Bosisio, and M. Moisan, IEEE J. Quantum Electron. **14**, 8 (1978).
[34]B. V. Derjaguin and D. V. Fedoseev, Surf. Coat. Technol. **38**, 131 (1989).
[35]D. R. Lide, *CRC Handbook of Chemistry and Physics*, 79th ed. (CRC, Boca Raton, FL, 1998).
[36]K. Karahashi, N. Yamagishi, T. Horikawa, and A. Toriumi, Proceedings of the American Vacuum Society 50th International Symposium, Baltimore, MD, 2003 (unpublished).
[37]K. Endo and T. Tatsumi, Jpn. J. Appl. Phys., Part 2 **42**, L685 (2003).
[38]S. Horii, K. Yamamoto, M. Asai, H. Miya, and M. Niwa, Jpn. J. Appl. Phys., Part 1 **42**, 5176 (2003).
[39]W. Wang, T. Nabatame, and Y. Shimogaki, Jpn. J. Appl. Phys., Part 1 **43**, L1445 (2004).

Redistribution subject to AVS license or copyright; see http://scitation.aip.org/termsconditions. Download to IP: 130.54.110.32 On: Mon, 25 Jan 2016 04:23:40